DALTON
FULL PAPER

Synthetic and structural studies of heteroleptic platinum(II) complexes containing crown trithioether and diphosphine ligands †

Gregory J. Grant,*[a] David F. Galas,[a] Ivan M. Poullaos,[a] Shawn M. Carter[a] and Donald G. VanDerveer[b]

[a] *Department of Chemistry, The University of Tennessee at Chattanooga, Chattanooga, TN 37403, USA*
[b] *School of Chemistry and Biochemistry, Georgia Institute of Technology, Atlanta, GA 30332, USA*

Received 18th March 2002, Accepted 10th June 2002
First published as an Advance Article on the web 11th July 2002

We wish to report the syntheses and spectroscopic properties of seven new Pt(II) heteroleptic complexes containing a series of diphosphine [P2 = $Ph_2PCH_2CH_2PPh_2$ (dppe), $Ph_2P(CH_2)_3PPh_2$ (dppp), $Ph_2P(CH_2)_4PPh_2$ (dppb), $Ph_2P(CH_2)_5PPh_2$ (dpppe), 1,2-$Ph_2PC_6H_4PPh_2$ (dppbe), and 1,2-$Ph_2C_2H_2PPh_2$ (dppv)] ligands and the crown trithioethers [9]aneS_3 (1,4,7-trithiacyclononane) or [10]aneS_3 (1,4,7-trithiacyclodecane). All seven reported complexes have the general formula [Pt([*n*]aneS_3)(P2)]$(PF_6)_2$ and form similar structures in which the Pt(II) center is surrounded by a *cis* arrangement of the two P donors from the diphosphine chelate and two sulfur atoms from the trithioether ligand. The third sulfur atom forms a longer interaction with the platinum resulting in an elongated square pyramidal structure with Pt–S axial distances ranging from 2.6505(9) to 2.8766(17) Å. The ^{195}Pt NMR chemical shifts for the complexes show values in the range of −4400 to −4700 ppm, consistent with a *cis*-PtS_2P_2 coordination sphere.

Introduction

A number of research groups have investigated the coordination chemistry of crown thioether ligands, such as 1,4,7-trithiacyclononane ([9]aneS_3), and work continues to progress in several areas including transition metal complexes, main group compounds, and organometallic complexes.[2] One particularly active area of focus involves thioether complexes of platinum(II) due to the high stability of Pt–S bonds and the relevance of this type of bond in catalysis and the pharmacodynamics of *cis*-platin.[3] These thioether complexes contain common, but unusual, structural features. They typically exhibit structures which involve a distorted square planar array of four equatorial sulfur donors around the Pt(II) center. However, there are usually additional long distance Pt–S interactions involving the third sulfur atom present in the coordinated trithioether. These long distance interactions result in complex structures best described as elongated square pyramids [S_4 + S_1] or elongated octahedra [S_4 + S_2].[4,5] The axial platinum–sulfur interactions have been described in a variety of ways (weak bonds, non-bonding interactions, agostic interactions, *etc*.), and their electronic nature is of considerable theoretical interest since they represent an intermediate case between bonding and non-bonding extremes.[6] Indeed, the six Pt–S axial distances reported here all lie between the covalent radius and the van der Waals radius of a platinum(II)–sulfur interaction.[7] It has been shown that these long distance Pt–S interactions result in unusual spectroscopic and electrochemical properties displayed by platinum–thioether complexes including visible *d*–*d* electronic transitions and a reversible Pt(II)/Pt(III) couple observed in cyclic voltammetric experiments. Additionally, the atypical Pt complex structures have been correlated with the conformational preferences of the individual crown thioether ligands.[6]

Although several homoleptic Pt(II) crown thioether complexes have now been structurally characterized, heteroleptic complexes with phosphine ligands are much less developed. Phosphine ligands are known to be effective and important catalysts, especially chiral diphosphines as asymmetric catalysts.[8] Phosphines have both stronger donor and accepting properties than thioethers so the mixed ligand complexes may have interesting electronic and structural properties. Some reports on mixed phosphine–sulfur ligand complexes have appeared, but work on crown thioethers such as [9]aneS_3 is limited.[9] It is interesting to note that the value of the P–M–P bite angle correlates well with catalytic reactions observed for a variety of diphosphine complexes, and we are interested in examining this feature in the presence of a coordinated crown thioether.[10] We have recently reported two initial studies dealing with phosphine–crown thioether Pt(II) complexes[11,12] which complement an earlier paper by Schröder and co-workers describing several related heteroleptic Pd(II) complexes.[13] We are interested in extending this research into crown thioether–diphosphine complexes to include Pt(II) since ^{195}Pt represents an attractive nucleus for NMR study. Important additional data to probe the ligand–Pt interactions can be provided by ^{31}P NMR chemical shifts and $^1J(^{195}Pt–^{31}P)$ couplings. Furthermore, due to their elongated square pyramidal structures, Pt(II) and Pd(II) complexes such as these have been used as models for ligand substitution reactions which proceed by associative mechanisms in four coordinate complexes.[14] Our report expands the series of related $[Pt([9]aneS_3)(P2)]^{2+}$ complexes to include diphosphine ligands containing from zero to five methylene carbon spaces. In that regard, we are now fully able to examine the effects that modifications in chelate ring size in a series of related diphosphine chelators have on their complexation behavior. A listing of the different ligand structures used in this report is given in Chart 1. We wish to report the syntheses and spectroscopic properties of seven new Pt(II) heteroleptic complexes containing a series of diphosphine [P2 = Ph_2PCH_2-CH_2PPh_2 (dppe), $Ph_2P(CH_2)_3PPh_2$ (dppp), $Ph_2P(CH_2)_4PPh_2$

† Heteroleptic platinum(II) complexes with crown thioether and phosphine ligands. Part IV.[1]

DOI: 10.1039/b202741k

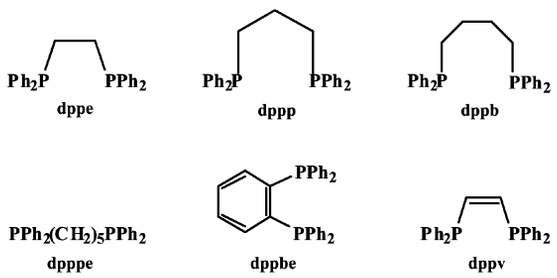

Chart 1

(dppb), $Ph_2P(CH_2)_5PPh_2$ (dpppe), 1,2-$Ph_2PC_6H_4PPh_2$ (dppbe), and 1,2-$Ph_2C_2H_2PPh_2$ (dppv)] ligands and the crown trithioethers [9]aneS_3 (1,4,7-trithiacyclononane) or [10]aneS_3 (1,4,7-trithiacyclodecane).

Results and discussion

Syntheses

A series of six new heteroleptic complexes containing achiral diphosphine (P2) ligands with the crown trithioether [9]aneS_3 are readily prepared from the dichloro complex [Pt([9]aneS_3)-Cl_2][15] by ligand substitution reactions and subsequently isolated as yellow–orange hexafluorophosphate salts. The general synthesis is illustrated in Scheme 1 for the dppe–[9]aneS_3 complex. These heteroleptic complexes have the general formulae [Pt([9]aneS_3)(P2)]$(PF_6)_2$, and using the same procedure, we have also prepared one [10]aneS_3 complex of the formula [Pt([10]aneS_3)(dppe)]$(PF_6)_2$. We would like to note that although the complete series of diphosphine complexes containing from zero ($2 \times PPh_3$) to five methylene spacers (dpppe) between the two phosphorus donors has now been successfully prepared, we were not able to synthesize the analogous mononuclear complex containing a diphosphine chelate with six methylene spacers ($PPh_2(CH_2)_6PPh_2$). This observation may reflect that six intervening methylene carbon spacers will position the two phosphorus donor atoms too far apart to chelate a single metal center. We have also been unable to prepare related complexes when the P2 ligand is the triphosphine ligand $(Ph_2PCH_2)_3CMe$ or when two PMe_3 monodentate ligands are present. In the case of $(Ph_2PCH_2)_3CMe$, the product showed a complex ^{31}P NMR spectrum indicating oxidation of some phosphorus donors as well as the presence of an uncoordinated ligand. In our attempt to prepare [Pt([9]aneS_3)-$(PMe_3)_2$)]$(PF_6)_2$, two different sets of crystals, one orange and one yellow–orange, were obtained suggesting that both the diphosphine and the chloro-monophosphine complexes were present.[1] Similar behavior has been observed for the two analogous Pd(II) complexes.[13]

The presence of the [9]aneS_3 and diphosphine ligands as well as uncoordinated hexafluorophosphate is confirmed *via* infrared spectroscopy, and the elemental analyses are consistent with the reported complex stoichiometries. The electronic spectra of the complexes are dominated by two charge transfer bands, the first one occurring near 380 nm and a second, much more intense band near 265 nm. The former is tentatively assigned as a $d\pi$ (Pt)$\longrightarrow\pi^*$ (diphosphine) MLCT transition while the latter is assigned as a $\pi\longrightarrow\pi^*$ transition of the diphosphine. The two transitions are red shifted relative to the analogous Pd(II) complexes.[13]

Proton and carbon-13 NMR spectroscopy

The proton and carbon-13 NMR spectra of all the complexes show the correct number of peaks, splittings, and intensities associated with the three basic components; four phenyl rings from the two PPh_2 moieties, the trithioether ligand, and the remaining proton or carbon atoms found in a particular diphosphine. In addition, ^{13}C DEPT experiments confirm all the carbon connectivities. The [9]aneS_3 region of the proton NMR spectrum appears as a characteristic AA′BB′ splitting pattern due to its twelve methylene protons.[11–14] For all of the complexes studied, the [9]aneS_3 ligand is fluxional resulting in a single ^{13}C NMR resonance for the six equivalent carbons. This phenomena has been observed in every known (now approximately 40 examples) [9]aneS_3 complex with Pt(II) and Pd(II), regardless of the ancillary ligand, and contrasts with their solid state structures which show elongated square pyramids or octahedra. The fluxionality arises from the rapid intramolecular exchange of the three sulfur atoms of the [9]aneS_3 ligands (1,4-metallotropic shift).[16] All of the ^{13}C resonances for the complexed [9]aneS_3 appear as a singlet downfield relative to the free ligand. In addition, two complexes (dpppe and dppv) show singlets that are shifted downfield by 2–3 ppm compared to the other Pt(II) complexes studied. The [10]aneS_3 ligand in [Pt([10]aneS_3)(dppe)]$(PF_6)_2$ is also fluxional as confirmed recently in two other Pt(II)–[10]aneS_3 complexes.[1,15] There is a noted distinction for the proton and carbon-13 chemical shifts involving the α-carbon of the diphosphine ligand in the $[Pt([9]aneS_3)(dppe)]^{2+}$ complex. In both spectra, a large downfield chemical shift is observed. For this particular complex, the dppe methylene resonance is downfield of the strong ^{13}C NMR [9]aneS_3 singlet while it is upfield for all the other diphosphine complexes. Similarly, its ^{1}H methylene resonance is shifted downfield by about 3 ppm relative to the diphosphine methylene protons in all other complexes and even appears downfield of the nitromethane solvent resonance. The AA′BB′ pattern in the proton spectrum of the [9]aneS_3 is also shifted downfield by 0.3 ppm relative to all of the other complexes.

In all complexes, the *ortho* and *meta* carbon atoms of the phenyl rings in the diphosphine show a complex splitting pattern, probably arising from longer range ^{13}C–^{31}P coupling while the *para* carbon appears as a singlet. The quaternary carbon adjacent to the phosphorus shows a non-first order spectrum with $^{1}J(^{13}C–^{31}P)$ coupling. Also, complex, but very similar, non-first order spectra with $^{1}J(^{13}C–^{31}P)$ couplings are observed for all α-methylene carbons in the dppe through dpppe series of homologous complexes. The β-methylene carbons in the dppp complex shows non-first order spectra with $^{2}J(^{13}C–^{31}P)$ couplings, but evidence for these same couplings is absent in the dppb and dpppe homologs. Interestingly, the γ-methylene carbon in the dpppe chelate ring shows evidence of $^{3}J(^{13}C–^{31}P)$ coupling even though its β-methylene carbons appear as a singlet. Thus, the observed phosphorus–carbon couplings in this series of diphosphine chelate rings appear to be enhanced or diminished by the conformation adopted by a particular ligand.

^{31}P and ^{195}Pt NMR spectroscopy

A summary of these NMR data appears in Table 1. For all the complexes reported here, the ^{31}P NMR spectrum consists of a sharp singlet showing the magnetic equivalence of the two phosphorus atoms of the diphosphine chelate. Due to the presence of both NMR active and non-active Pt centers (^{195}Pt,

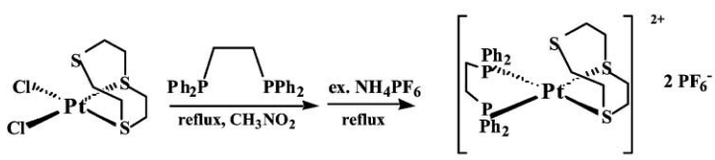

Scheme 1

Table 1 ^{195}Pt and ^{31}P NMR data for heteroleptic Pt(II) crown thioether–diphosphine complexes. All complexes contain a *cis*-PtS_2P_2 structure

Complex	δ ^{195}Pt (ppm)	δ ^{31}P (ppm)	$^1J(^{195}Pt–^{31}P)$/Hz	Ref.
$[Pt([9]aneS_3)(dppe)]^{2+}$	−4069	−51.56	2740	Present work (PW)
$[Pt([9]aneS_3)(dppp)]^{2+}$	−4478	−8.52	3069	PW
$[Pt([9]aneS_3)(dppb)]^{2+}$	−4497	10.74	3211	PW
$[Pt([9]aneS_3)(dpppe)]^{2+}$	−4426	−11.35	3239	PW
$[Pt([9]aneS_3)(dppbe)]^{2+}$	−4568	46.07	3202	PW
$[Pt([10]aneS_3)(dppe)]^{2+}$	−4602	35.16	3219	PW
$[Pt([9]aneS_3)(dppv)]^{2+}$	−4681	42.09	3219	PW
$[Pt([9]aneS_3)(dppm)]^{2+}$	−4601	50.50	3188	11
$[Pt([9]aneS_3)(PPh_3)_2]^{2+}$	−4399	12.03	3365	11
$[Pt([9]aneS_3)(dppf)]^{2+}$	−4353	15.09	3499	12

I = ½, 33.8%), a doublet of ^{195}Pt satellites appears in the ^{31}P NMR spectrum of the Pt complexes. The values of the $^1J(^{195}Pt–^{31}P)$ coupling constants are *ca.* 3200 Hz for all of the new complexes except two. The coupling constants indicate a *cis* arrangement of two phosphorus and two sulfur donors around the platinum(II) center. Interestingly, the observed trend in ^{195}Pt–^{31}P coupling constants is dppe < dppp < dppm (bis(diphenylphosphino)methane), opposite to the one observed when chloride is the ancillary ligand. The values further show substantially reduced $^1J(^{195}Pt–^{31}P)$ coupling in the thioether complexes.[17] We suggest that the relative differences between the *trans* effects for the crown thioether and the chloride ligands are responsible for the reversed trend and decreased coupling values. The dppe complex shows a surprisingly small ^{195}Pt–^{31}P coupling (2740 Hz), 500 Hz smaller than the typical diphosphine value. We propose that lower ring strain in the five-membered chelate of the dppe complex lowers the coupling dramatically. Similarly, due to the modest ring strain in its six-membered chelate ring, the dppp complex also shows a coupling constant (3069 Hz) which is smaller than the other diphosphine complexes.

With the exception of one diphosphine ligand, all of the ^{195}Pt NMR chemical shifts presented in Table 1 appear between −4400 and −4700 ppm with the anticipated triplet splitting pattern of an AX_2 spin system. These spectra are indicative of a *cis*-PtP_2S_2 coordination sphere. The lone exception is again the dppe complex which shows a Pt(II) center that is deshielded by several hundred ppm (−4069). Interestingly, this chemical shift falls almost at the arithmetic mean between the ^{195}Pt NMR chemical shifts for $[Pt([9]aneS_3)Cl_2]$ and $[Pt(dppe)Cl_2]$ (−3605 ppm and −4554 ppm, respectively).[15,18] Also, the chemical shift is quite comparable to the values we have just reported for *cis*-$PtPClS_2$ coordination spheres (~ −4090 ppm).[1] We propose that the unusual downfield chemical shift arises from the lower ring strain within the five-membered dppe ring chelate. The complex $[Pt([10]aneS_3)(dppe)]^{2+}$ also shows a relatively deshielded Pt(II) center. In contrast, the two complexes involving unsaturated diphosphine ligands, dppbe and dppv, show a highly shielded platinum nucleus. Enhanced π bonding between the Pt and the unsaturated diphosphine chelate could be the source of the upfield ^{195}Pt NMR chemical shift, an observation seen in other dppv complexes.[19] The complexes also show a deshielded phosphorus nucleus and relatively large $^1J(^{195}Pt–^{31}P)$ coupling constants, both consistent with a stronger P–Pt interaction. Our results from ^{195}Pt NMR spectroscopy show how the electronic and steric properties of the diphosphine influence the interaction with the platinum center.

The ^{31}P NMR chemical shifts of the complexes presented here range from −50.50 to 46.07 ppm and show the expected doublet of ^{195}Pt satellites. The two dppe complexes show the most upfield ^{31}P resonances. There is a substantial 100 ppm ^{31}P NMR upfield chemical shift in going from our previously reported diphosphine complex, $[Pt([9]aneS_3)(dppm)]^{2+}$, to the analogous dppe complex, resulting from ring strain differences between the highly strained four-membered chelate ring in the dppm and the relatively strain free dppe five-membered chelate ring.[11] In fact, the ^{31}P NMR chemical shift in $[Pt([9]aneS_3)(dppe)]^{2+}$ is shifted by 40 ppm upfield compared to the free dppe ligand while the dppm resonance is shifted by 60 ppm downfield in its $[9]aneS_3$ complex relative to the dppm ligand. Diphosphine ligands like dppm, which are both good σ donors and contain small bite angles, result in more thermodynamically stable Pt(II) complexes.[21] Also, the ^{195}Pt NMR spectrum of the dppm complex shows a highly shielded platinum(II) nucleus, and a relatively easily reduced Pt center in its electrochemical behavior. As noted, the two complexes involving unsaturated diphosphine ligands, dppbe and dppv, also show a deshielded phosphorus nucleus so there is a general inverse correlation between the ^{195}Pt and ^{31}P NMR chemical shifts. Among the diphosphine complexes, the lower ring strain for the dppe chelate results in a smaller ^1J platinum–phosphorus coupling, a deshielded Pt nucleus, and a shielded P nucleus.

The replacement of chloride donors by the crown thioether $[9]aneS_3$ provides for an interesting direct comparison between $[Pt(dppe)Cl_2]$ and $[Pt([9]aneS_3)(dppe)]^{2+}$. The thioether–phosphine complex shows a platinum nucleus which is deshielded by about 500 ppm compared to the chloride complex. In addition, replacement of the two chloride ligands by the thioether results in a 90 ppm upfield ^{31}P NMR chemical shift and a reduction in $^1J(^{195}Pt–^{31}P)$ of almost 900 Hz. The second thioether–dppe complex included in our report, $[Pt([10]aneS_3)(dppe)]^{2+}$, also shows a similar trend in NMR data although the differences are not as great as with the smaller trithioether. All of these data are consistent with a weakening of the platinum–phosphorus interaction when a thioether has replaced a chloride donor. We believe that the π donor–acceptor abilities of the $[9]aneS_3$ ligand are the source of this weakening, and there is increasing data to support the view that crown thioethers have moderate π donor–acceptor properties.[20]

Structural studies

Selected bond distances and bond angles for the six crystal structures reported in this work are given in Table 2, and a series of ORTEP perspectives for the complex cations are shown in Figs. 1–6. All six structures form what are best described as elongated square pyramids with *cis*-S_2P_2 + S_1 coordination involving two equatorial Pt–S bonds and Pt–P bonds. The third sulfur from the crown trithioether interacts with the metal ion albeit from a much longer distance to "cap" the square plane around the platinum center. In the six structures, the Pt–S equatorial bonds show only modest variations in length and range from 2.3432(11) to 2.3995(6) Å. The platinum–phosphorus bonds are shorter than the Pt–S bonds, and they range from 2.2555(15) to 2.3087(7) Å. Due to the relative *trans* effects for the donor atoms found in the square plane, the shorter Pt–S bond *always* lies *trans* to the longer Pt–P bond. This structural result is consistent with our hypothesis that the presence of the trithioether ligand weakens the platinum–phosphine interaction.

The axial Pt–S distances show a much greater variation than do their equatorial analogs, ranging from 2.6506(9) to 2.8766(11) Å. In general, the Pt–S axial distance increases with

Table 2 Selected bond distances (Å) and angles (°) for [Pt([9]aneS$_3$)(dppe)](PF$_6$)$_2$ (**1**), [Pt([9]aneS$_3$)(dppp)](PF$_6$)$_2$ (**2**), [Pt([9]aneS$_3$)(dppb)](PF$_6$)$_2$ (**3**), [Pt([9]aneS$_3$)(dpppe)](PF$_6$)$_2$ (**4**), [Pt([9]aneS$_3$)(dppbe)](PF$_6$)$_2$ (**5**), and [Pt([10]aneS$_3$)(dppe)](PF$_6$)$_2$ (**6**)

	1	**2**	**3**	**4**	**5**	**6**
Pt–S_{eq}	2.3685(15), 2.3662(17)	2.3679(13), 2.3624(15)	2.3749(6), 2.3995(6)	2.3686(17), 2.3794(15)	2.3432(11), 2.3794(11)	2.3621(9), 2.3676(9)
Pt–S_{axial}	2.737(2)	2.805(1)	2.8487(7)	2.8766(17)	2.7180(12)	2.6505(9)
Pt–P_{eq}	2.2555(15), 2.2570(16)	2.2780(13), 2.2796(15)	2.2896(7), 2.3087(7)	2.3007(17), 2.3053(15)	2.2559(12), 2.2729(11)	2.2707(9), 2.2730(9)
P–P distance	3.030(2)	3.3340(1)	3.453(6)	3.5130(17)	3.1160(11)	3.0910(9)
S_{eq}–Pt–S_{eq}	88.30(6)	87.54(5)	87.32(2)	86.65(5)	86.93(4)	94.51(3)
P(1)–Pt–P(2)	84.36(6)	94.29(5)	97.38(2)	99.41(5)	87.68(5)	85.73(3)
P(1)–Pt–S_{eq}	168.79(6) 92.73(6)	168.75(5), 87.06(5)	164.90(2), 84.18(2)	169.31(5), 87.87(6)	166.77(5), 88.20(4)	174.75(3), 87.40(3)
P(2)–Pt–S_{eq}	169.75(6), 92.67(6)	166.60(6), 88.72(5)	170.50(2), 89.03(2)	165.52(6), 84.07(5)	172.19(4), 95.72(5)	165.77(4), 91.32(3)
S_{eq}–Pt–S_{axial}	83.86(6), 83.52(6)	83.673(5), 82.667(5)	81.89(2), 82.66(2)	82.13(6), 81.37(5)	86.11(4), 84.02(4)	85.58(3), 84.62(3)

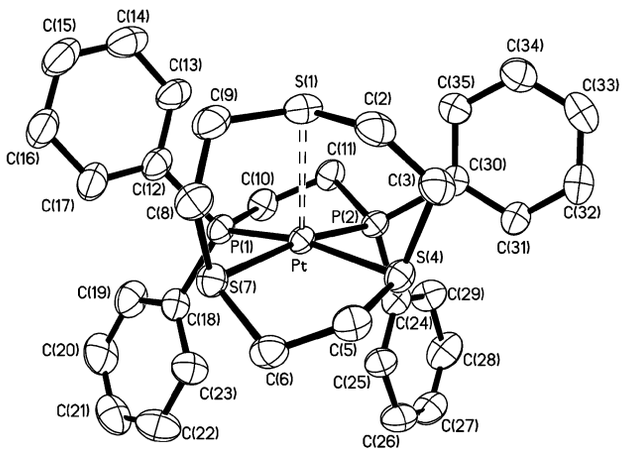

Fig. 1 ORTEP perspective of cation in [Pt([9]aneS$_3$)(dppe)](PF$_6$)$_2$ (**1**).

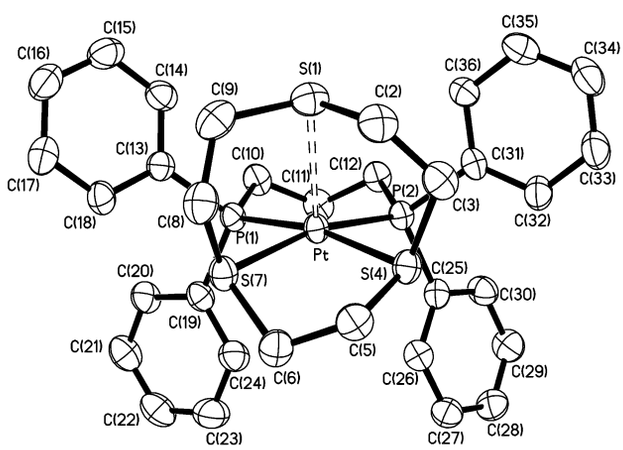

Fig. 2 ORTEP perspective of cation in [Pt([9]aneS$_3$)(dppp)](PF$_6$)$_2$ (**2**).

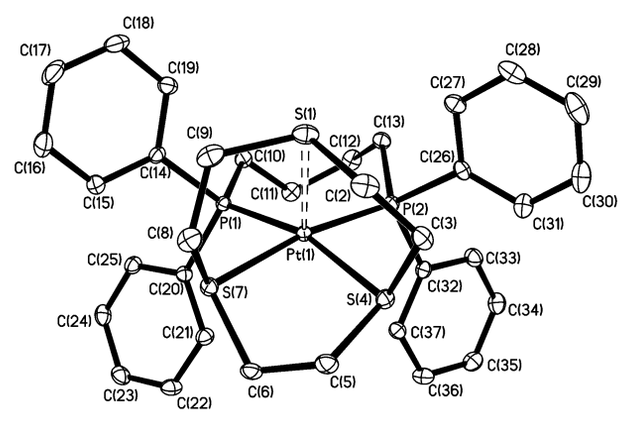

Fig. 3 ORTEP perspective of cation in [Pt([9]aneS$_3$)(dppb)](PF$_6$)$_2$ (**3**).

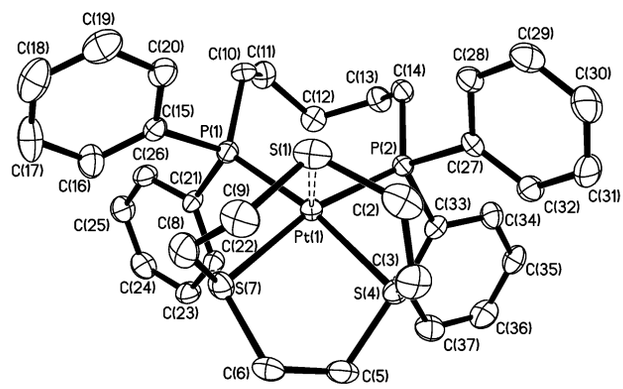

Fig. 4 ORTEP perspective of cation in [Pt([9]aneS$_3$)(dpppe)](PF$_6$)$_2$ (**4**).

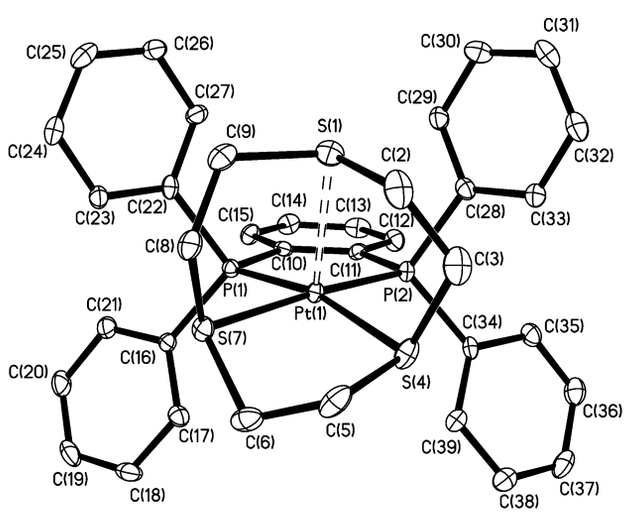

Fig. 5 ORTEP perspective of cation in [Pt([9]aneS$_3$)(dppbe)](PF$_6$)$_2$ (**5**).

the increasing size of the P–Pt–P angle so that the dpppe complex exhibits the largest value. All of these values are much smaller than 3.5 Å, the sum of the van Der Waals radii and confirm that a long distance Pt–S interaction is occurring.[9] The degree of this interaction is dependent upon the particular diphosphine that is present, but note that the shorter distances begin to approach values associated with platinum–sulfur covalent bonds (2.4 Å). We have recently shown for a series of related complexes how the identity of the ancillary ligand can radically alter the Pt–S axial distances in the [Pt([9]aneS$_3$)] moiety, even by as much as 1 Å.[11] The axial distances in diphosphine complexes are the shortest observed for any ancillary ligand due to a combination of their charge and donor–acceptor properties.

A strong linear correlation exists between the $^1J(^{195}Pt–^{31}P)$ coupling constants and the P–Pt–P chelate bite angle for the four methylene diphosphine complexes presented in this

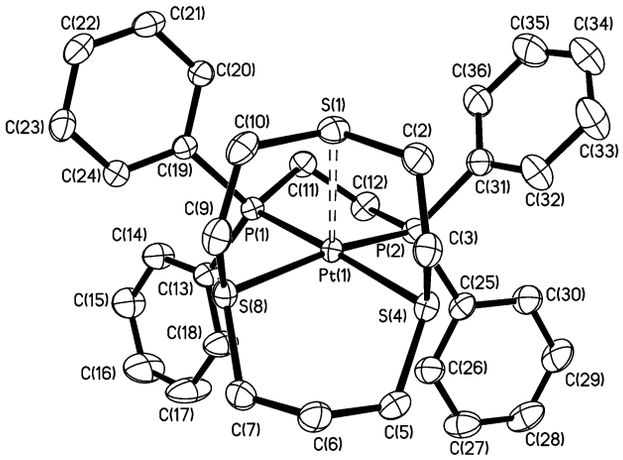

Fig. 6 ORTEP perspective of cation in $[Pt([10]aneS_3)(dppe)](PF_6)_2$ (**6**).

work.[22] A similar correlation between the same coupling and the Pt–P–C angle is also observed. We propose that these spectroscopic correlations arise from the specific conformation adopted by the diphosphine chelate rings. The magnitude of the phosphorus–platinum coupling constant is dominated by the Fermi contact term which is greatly affected by the variations of these two angles in the complexes.[17] The correlations between the P–Pt–P chelate bite angle and the selectivity of diphosphine catalysts in such reactions as hydroformylation and cross-coupling have previously been noted, and the $^1J(^{195}Pt–^{31}P)$ coupling constants appear to provide an important experimental probe for this structural feature.[10] As one progresses through the dppe > tdppp > dppb > dpppe series, there is a steady increase in the P–Pt–P chelate angle as the number of methylene spacers increases. Note there is a commensurate decrease in the S–Pt–S chelate angle of $[9]aneS_3$. Our results show how the identity and conformation of the ancillary diphosphine ligand can influence structural changes within the coordinated $[9]aneS_3$ ligand. In contrast, there is no strong correlation between the ^{195}Pt or ^{31}P NMR chemical shifts and diphosphine chelate ring size for the complexes studied here.

Among the six structures presented here, the $[9]aneS_3$–dppe complex shows the shortest average bond distances for both the Pt–S (2.367(5) Å) and Pt–P (2.256(5) Å) bonds. Due to the formation of a five-membered chelate ring by the dppe donor, the S_{eq}–Pt–S_{eq} chelate angle is closest to 90° in this complex and thus shows the least chelate ring strain of any ligand included in this work. The two dppe phosphorus atoms approach each other the closest and have the P–Pt–P "bite" angle closest to 90°. The bite angle is about 2° larger than the average value of 82.55° reported for dppe complexes, a consequence of the trithioether ligand.[10] We noted earlier the unusual NMR chemical shifts and couplings shown by this particular complex. In the dppp complex, the six-membered chelate ring of the dppp adopts a twist-boat conformation. Interestingly, the dppb complex shows the longest equatorial Pt–S and Pt–P bonds of this series. The dppp and dppb complexes show increases in the P–Pt–P chelate angles of 2.73° and 0.31°, respectively, compared to average values reported for other complexes involving these two diphosphines.[10] In the complex $[Pt([9]aneS_3)(dpppe)](PF_6)_2$, the dpppe ligand functions as a bidentate ligand to a single Pt(II) center to form an uncommon eight-membered chelate ring.[23] Due to the presence of the five methylene carbons, the two phosphorus donors are spread wide apart (3.5130(17) Å) resulting in a large P–Pt–P angle of 99.41(5)° and a small S–Pt–S bite angle of 86.65(5)°. The Pt–P bond distances increase with increasing chelate bite angle of the diphosphine so that this complex also has the longest platinum–phosphine bonds.

Like the other complexes, $[Pt([9]aneS_3)(dppbe)](PF_6)_2$ forms an elongated square pyramidal structure [S_2P_2 + S_1], with platinum–sulfur equatorial distances of 2.3432(11) and 2.3794(11) Å and phosphine–platinum distances of 2.2559(12) and 2.2729(11) Å. The third sulfur from the $[9]aneS_3$ (S1) interacts from a much longer distance of 2.7180(12) Å. The dppbe complex contains the shortest Pt–P equatorial distances of the six structures reported here, a consequence of the enhancement of the π interaction between the platinum and the unsaturated diphosphine. This π interaction is also seen in relatively short Pt–S equatorial distances, but more importantly, in its short Pt–S axial distance. Indeed, the dppbe complex exhibits the shortest Pt–S axial interaction of any in the $[9]aneS_3$ series and has the shortest average bond lengths among all four bonds. Even though both dppe and dppbe form five-membered chelate rings, the P–P distances are shorter than for the dppe complex due to the greater conformational flexibility found in the ethylene-bridged diphosphine. However, electronic factors result in the dppbe complex having a more shielded Pt nucleus, a more deshielded P nucleus, and a relatively large Pt–P coupling. The dppbe complex also differs from the methylene diphosphine complexes in that the P–Pt–P chelate angle has decreased by over 5° compared to average values of other dppbe complexes.[10] In contrast, the trithioether complexes with methylene diphosphine chelates all show relatively large P–Pt–P chelate angles.

The structure of the complex $[Pt([10]aneS_3)(dppe)](PF_6)_2$ provides an interesting comparison to its $[9]aneS_3$ analog since both contain the identical diphosphine chelator. The most noticeable feature of the $[10]aneS_3$ structure is its short Pt–S axial distance (2.6505(9) Å), by far the smallest among this group of six, and among the shortest observed in any platinum–crown thioether complex.[15] Due to the greater flexibility of the $[10]aneS_3$ ligand, axial Pt–S distances in $[10]aneS_3$–Pt complexes are often shorter than those found in their $[9]aneS_3$ counterparts as we have observed here. The Pt–S equatorial distances, however, are remarkably similar to those found in the $[9]aneS_3$–dppe complex as well as for the other structures. In contrast, the Pt–P distances in the dppe have lengthened by about 0.02 Å. The internal S–Pt–S chelate angles have increased by about 7° in the $[10]aneS_3$ structure, a consequence of $[10]aneS_3$ forming a six-membered ring chelate as opposed to the five-membered ring in the $[9]aneS_3$ structure. The P–Pt–P bite angle has increased to 85.73(3)°, larger than the dppe bite angle in the $[9]aneS_3$ complex, and over 3° larger than the average value in a dppe complex. Our data suggest that the larger chelate ring angle of the trithioether ligand does have an effect on the structure of the diphosphine chelate. There are six reported structures of Pt(II) complexes involving $[10]aneS_3$ ligands, but this is only the second to form a stereoisomer which contains a six-membered chelate ring as opposed to a five-membered ring.[4,5,24] In both of these cases, the S–Pt–S chelate ring angle had expanded beyond 90° while structures containing five-membered chelate rings show angles less than 90°. The conformation adopted by the $[10]aneS_3$ ligand in the crystal structure is the [2323] conformation, and the same conformation is adopted by the ligand in several of the previously reported structures of its complexes.[2,24] In this conformation the six-membered chelate ring is found in the chair form.

The structure of $[Pt([9]aneS_3)(dppe)](PF_6)_2$ completes an important series along with the previously reported $[Pt(dppe)Cl_2]$ and $[Pt([9]aneS_3)Cl_2]$.[15,25] Consistent with our NMR data which shows a weakening of the platinum–phosphine interaction in the presence of the thioether ligand, the Pt–P bond distances in the dppe ligand have indeed lengthened from an average of 2.227(2) Å to an average of 2.256(2) Å when the chloride ligands are replaced by a thioether. Furthermore, the Pt–S bonds are shortened when the ancillary ligand present is a chloride or another halide (average = 2.25 Å) as opposed to a diphosphine. The average Pt–S bond distances for the diphosphine complexes presented here are about 2.37 Å. Consistent

with an enhanced π platinum–thioether equatorial interaction, the Pt–Cl bond lengths in [Pt([9]aneS$_3$)Cl$_2$] are shorter by over 0.025 Å than those in [Pt(dppe)Cl$_2$] (average: 2.328(4) *vs.* 2.355(2) Å).[15,25] It is interesting to note that of the approximately twenty crystal structures of Pt(II)–[9]aneS$_3$ complexes, those which contain the shortest Pt–S equatorial bonds also typically contain the longest Pt–S axial interactions and *vice versa*.[26]

The unusual metal–sulfur axial interactions arise from the interplay between the conformational requirements of the trithioether ligand and the electronic requirements of the Pt(II) or Pd(II) center. Previously, a primary focus in the examination of the axial interaction has been on the ability of the ancillary ligand to function as a π acceptor and thereby increase the positive charge on the metal center, causing the axial sulfur to be drawn closer to it. However, the diphosphine structures presented in this report contain Pt–S axial distances distinctly shorter than those found in complexes such as [Pt(9S3)(phen)]$^{2+}$, despite diphosphines being poorer π acceptors than diimine ligands like phenanthroline.[14] It may be possible that, through its donor–acceptor properties, the ancillary ligand can decrease or increase the Pt–S equatorial distances of the crown thioether. However, due to the rigid structure of a crown trithioether like [9]aneS$_3$, its axial sulfur is accordingly positioned closer or further from the platinum center. The importance of steric properties within the Pt(II)–thioether complexes does appear to have a role that has been neglected previously. Thus, it is through a combination of the steric and electronic properties of both the trithioether crown as well as the ancillary ligand that the unusual square pyramidal structures observed in these trithioether complexes are generated.

Conclusions

Seven new Pt(II) heteroleptic complexes containing a series of diphosphine ligands and the crown trithioethers [9]aneS$_3$ (1,4,7-trithiacyclononane) or [10]aneS$_3$ (1,4,7-trithiacyclodecane) with the general formula [Pt([*n*]aneS$_3$)(P2)](PF$_6$)$_2$ were synthesized. All the complexes form similar structures in which the Pt(II) center is surrounded by a *cis* arrangement of the two P donors from the diphosphine chelate and two sulfur atoms from the trithioether ligand. The third sulfur in every complex forms a longer axial interaction with the platinum resulting in an elongated square pyramidal structure with Pt–S axial distances ranging from 2.6505(9) to 2.8766(17) Å. These distances are among the shortest reported for Pt(II) complexes with crown trithioethers, and the distances are shorter than those observed with stronger π accepting ligands such as phenanthroline. The dpppe ligand chelates the Pt(II) ion to form an uncommon eight-membered chelate ring while the [10]aneS$_3$ ligand forms a linkage isomer with a six-membered chelate ring. The ^{195}Pt NMR chemical shifts for all complexes show values in the range of −4400 to −4700 ppm, consistent with a *cis*-PtS$_2$P2 coordination sphere. The values of the ^{31}P NMR chemical shifts and $^1J(^{195}\text{Pt}–^{31}\text{P})$ coupling constants further support the structural assignments, and dramatic differences are seen in the multinuclear NMR spectra of [Pt([9]aneS$_3$)(dppe)](PF$_6$)$_2$ due to reduced chelate ring strain. Among the four [9]aneS$_3$ complexes containing methylene diphosphines, there is a strong correlation between the $^1J(^{195}\text{Pt}–^{31}\text{P})$ coupling constants and the P–Pt–P bite angle. Differences in NMR spectroscopic and structural data between thioether–diphosphine complexes and chloride–diphosphine complexes can be related to the reduced Pt–P interaction in the thioether complexes due to the relative π donor–acceptor differences between the two classes of ligands. This report represents a systematic study of how the effects of chelate ring size and other structural changes within a range of diphosphine ligands may be monitored using the structural and spectroscopic properties of heteroleptic platinum(II) thioether complexes.

Experimental

All solvents and reagents were purchased from Aldrich Chemical Company and used as received. The starting complexes [Pt([9]aneS$_3$)Cl$_2$] and [Pt([10]aneS$_3$)Cl$_2$] were prepared following the published methods.[15] Elemental analyses were performed by Atlantic Microlab, Inc. of Atlanta, Georgia. Fourier transform infrared spectra were obtained as KBr powders using a Galaxy FT IR 5000 spectrophotometer equipped with an ATR accessory. Ultraviolet-visible spectra were obtained in acetonitrile using a Varian DMS 200 UV-visible spectrophotometer (molar absorption coefficients are given in dm^3 mol^{-1} cm^{-1}). ^{13}C{^{1}H} and ^{1}H NMR spectra were recorded on a Varian Gemini 300 NMR spectrometer using CD_3NO_2 for both the deuterium lock and reference. All observed carbon resonance connectivities were confirmed *via* DEPT (Distortionless Enhancement by Polarization Transfer) experiments. Platinum-195 NMR spectra (proton-decoupled) were recorded near 64.208 MHz using aqueous solutions of [PtCl$_6$]$^{2-}$ (0 ppm) as an external reference and a delay time of 0.01 seconds. Referencing was verified *versus* authentic samples of [PtCl$_4$]$^{2-}$ which was found to have a chemical shift at −1626 ppm, in agreement with the reported value of −1624 ppm.[27] Phosphorus-31 NMR spectra (proton-decoupled) were measured at 121.470 MHz, and referencing was done using phosphoric acid (0 ppm) as an external standard.[28]

Syntheses

General procedure. A mixture containing equal equivalents of [Pt([*n*]aneS$_3$)Cl$_2$] and the appropriate diphosphine was refluxed in 50–100 mL of CH_3NO_2 for 1–24 h. The resulting solution was allowed to cool slightly before two equivalents of NH_4PF_6 were added, and the mixture was refluxed for an additional 30 min. The solution was filtered whilst hot and concentrated on a rotary evaporator to less than $\frac{2}{3}$ its original volume. Ether was then diffused into the concentrate resulting in a yellow crystalline product as the hexafluorophosphate salt.

[Pt([9]aneS$_3$)(dppe)](PF$_6$)$_2$ (1). A mixture of [Pt([9]aneS$_3$)Cl$_2$] (93.0 mg, 0.208 mmol) and dppe (83.0 mg, 0.208 mmol) was refluxed in 50 mL of CH_3NO_2 for 1 h. Metathesis to the hexafluorophosphate salt and ether diffusion resulted in yellow crystals of [Pt([9]aneS$_3$)(dppe)](PF$_6$)$_2$ (147 mg, 138 mmol, 66.3%) suitable for X-ray diffraction (Found: C, 35.90; H, 3.49; S, 8.93. Calcd for $C_{32}H_{36}F_{12}P_4PtS_3$: C, 36.13; H, 3.41; S, 9.04%). IR: 3075, 3050, 2976, 2973, 2971, 2969, 1620, 1482, 1442, 1398, 1375, 1185, 837 (s, PF$_6^-$), 756, 702, 648, 652 cm^{-1}. Electronic spectrum (MeCN): λ_{max} at 383 nm (ε = 710) and at 263 nm (ε = 20000). ^{1}H-NMR (CD_3NO_2), δ (ppm): P*Ph*$_2$: 7.85, 7.64, 7.42 (m, 20 H); PC*H*$_2$C*H*$_2$P: 5.34 (m, 4 H); [9]aneS$_3$: complex AA′BB′ pattern at 3.11 and 2.88 ppm (12 H). ^{13}C{^{1}H}-NMR (CD_3NO_2), δ (ppm): P*Ph*$_2$: 135.2 (s, 4 C), 134.6 (m, 8 C), 131.8 (m, 8 C), 129.2 (m, 4 C); P*C*H$_2$*C*H$_2$P: 43.4 (m, 2 C, $^1J(^{13}\text{C}–^{31}\text{P})$ = 69 Hz); [9]aneS$_3$: 37.8 (s, 6 C). ^{195}Pt{^{1}H}-NMR (CD_3NO_2), δ ($\nu_{½}$): triplet at −4069 ppm (41 Hz) ($^1J_{PtP}$ = 2740 Hz). ^{31}P{^{1}H}-NMR (CD_3NO_2), δ: singlet at −51.75 ppm with ^{195}Pt satellites, ($^1J_{PtP}$ = 2740 Hz).

[Pt([9]aneS$_3$)(dppp)](PF$_6$)$_2$ (2). A mixture of [Pt([9]aneS$_3$)Cl$_2$] (100 mg, 0.224 mmol) and dppp (92.5 mg, 0.224 mmol) was refluxed in 50 mL of CH_3NO_2 for 1 h. Metathesis to the hexafluorophosphate salt and ether diffusion resulted in yellow crystals of [Pt([9]aneS$_3$)(dppp)](PF$_6$)$_2$ (131 mg, 0.122 mmol, 54.2%) which were suitable for X-ray diffraction (Found: C, 36.74; H, 3.62; S, 8.82, Calcd for $C_{33}H_{38}F_{12}P_4PtS_3$: C, 36.77; H, 3.55; S, 8.92%). IR: 3067, 3065, 3060, 3057, 2991, 2988, 2983, 2860, 1486, 1242, 1175, 1020, 1010, 842 (s, PF$_6^-$), 777, 651, 643, 592, 588 cm^{-1}. Electronic spectrum (MeCN): two λ_{max}

at 378 nm (ε = 350) and at 261 nm (ε = 22000). ^{1}H-NMR (CD_3NO_2), δ (ppm): PPh_2: 7.77, 7.63 (m, 20 H); PCH_2CH$_2$-CH_2P: 3.43 (m, 4 H); [9]aneS$_3$: complex AA′BB′ pattern at 2.84 and 2.45 (12 H); PCH$_2$CH_2CH$_2$P: 2.28 (m, 2 H). ^{13}C{^{1}H}-NMR (CD_3NO_2), δ (ppm): PPh_2: 135.3 (m, 8 C), 135.1 (s, 8 C), 131.5 (m, 8 C), 129.2 (m, 4 C); [9]aneS$_3$: 38.2 (s, 6 C); PCH$_2$CH$_2$-CH_2P: 27.9 (m, 2 C); PCH$_2$CH_2CH$_2$P: 21.6 (m, 1 C). ^{195}Pt{^{1}H}-NMR (CD_3NO_2), δ ($\nu_{1/2}$): triplet at −4478 ppm (34 Hz) ($^1J_{PtP}$ = 3073 Hz). ^{31}P{^{1}H}-NMR (CD_3NO_2), δ: singlet at −8.52 ppm with ^{195}Pt satellites ($^1J_{PtP}$ = 3069 Hz).

[Pt([9]aneS$_3$)(dppb)](PF$_6$)$_2$ (3). A mixture of [Pt([9]aneS$_3$)Cl$_2$ (94.0 mg, 0.211 mmol) and dppb (101 mg, 0.237 mmol) was refluxed in 50 mL of CH_3NO_2 for 2.5 h. Metathesis to the hexafluorophosphate salt and ether diffusion resulted in yellow crystals of [Pt([9]aneS$_3$)(dppb)](PF$_6$)$_2$ (121 mg, 0.111 mmol, 52.6%) which were suitable for X-ray diffraction (Found: C, 37.29; H, 3.74; S, 8.67. Calcd for $C_{34}H_{40}F_{12}P_4PtS_3$: C, 37.40; H, 3.69; S, 8.81%). IR: 3072, 3052, 2970, 2941, 2923, 1625, 1437, 1395, 1187, 840 (s, PF$_6^-$), 750, 699, 643 cm^{-1}. Electronic spectrum (MeCN): two λ_{max} at 380 nm (ε = 350) and at 263 nm (ε = 21000). ^{1}H-NMR (CD_3NO_2), δ (ppm): PPh_2: 7.87, 7.63 (m, PPh$_2$, 20 H); PCH_2CH$_2$CH$_2$CH_2P: 3.33 (m, 4 H); [9]aneS$_3$: complex AA′BB′ pattern at 2.86 and 2.42 (12 H); PCH$_2$CH_2-CH_2CH$_2$P: 1.86 (m, 4 H). ^{13}C{^{1}H}-NMR (CD_3NO_2), δ (ppm): PPh_2: 134.5 (m, 8 C), 134.2 (s, 4 C); 130.7 (m, 8 C), 129.8 (m, 4 c); [9]aneS$_3$: 37.2 (s, 6 C); PCH$_2$CH$_2$CH$_2$CH_2P: 30.4 (m, 2 C); PCH$_2$CH_2CH_2CH$_2$P: 22.5 (s, 2 C). ^{195}Pt{^{1}H}-NMR (CD_3NO_2), δ ($\nu_{1/2}$): triplet at −4497 ppm (53 Hz) ($^1J_{PtP}$ = 3207 Hz). ^{31}P{^{1}H}-NMR (CD_3NO_2), δ: singlet at 10.74 ppm with ^{195}Pt satellites ($^1J_{PtP}$ = 3211 Hz).

[Pt([9]aneS$_3$)(dpppe)](PF$_6$)$_2$ (4). A mixture of [Pt([9]aneS$_3$)-Cl$_2$] (90.0 mg, 0.202 mmol) and dpppe (89.0 mg, 0.202 mmol) was refluxed in 100 mL of CH_3NO_2 for 2 hours. Metathesis to the hexafluorophosphate salt and ether diffusion resulted in yellow crystals of [Pt([9]aneS$_3$)(dpppe)](PF$_6$)$_2$ (135 mg, 0.122 mmol, 60.4%) which were suitable for X-ray diffraction (Found: C, 38.01; H, 3.83; S, 8.79. Calcd for $C_{36}H_{42}F_{12}P_4PtS_3$: C, 38.01; H, 3.83; S, 8.70%). IR: 3079, 3050, 3045, 2970, 2942, 2933, 2861, 1625, 1501, 1439, 1395, 1306, 1187, 841 (s, PF$_6^-$), 750, 699, 643, 564 cm^{-1}. Electronic spectrum (MeCN): two λ_{max} at 382 nm (ε = 420) and at 270 nm (ε = 27000). ^{1}H-NMR (CD_3NO_2), δ (ppm): PPh_2: 7.88. 7.69 (m, 20 H); PCH_2CH$_2$-CH$_2$CH$_2$CH_2P: 3.33 (m, 4H); [9]aneS$_3$: complex AA′BB′ pattern at 2.82 and 2.37 (12 H); PCH$_2$CH_2CH$_2$CH_2CH$_2$P: 1.84 (m. 4H); PCH$_2$CH$_2$CH_2CH$_2$CH$_2$P 1.55 (m, 2H). ^{13}C{^{1}H}-NMR (CD_3NO_2), δ (ppm): PPh_2: 134.7 (m, 8 C), 134.3 (s, 4 C), 131.1 (m, 8 C), 130.9 (m, 4 C); [9]aneS$_3$: 35.8 (s, 6 C); PCH$_2$CH$_2$CH$_2$-CH$_2$CH_2P: 30.1 (m, 2 C); PCH$_2$CH_2CH$_2$CH_2CH$_2$P: 25.7 (s, 2 C); PCH$_2$CH$_2$CH_2CH$_2$CH$_2$P: 23.0 (m, 2 C). ^{195}Pt{^{1}H}-NMR (CD_3NO_2), δ ($\nu_{1/2}$): triplet at −4429 ppm (160 Hz) ($^1J_{PtP}$ = 3244 Hz). ^{31}P{^{1}H}-NMR (CD_3NO_2), δ: singlet at −11.35 ppm with ^{195}Pt satellites ($^1J_{PtP}$ = 3239 Hz).

[Pt([9]aneS$_3$)(dppbe)](PF$_6$)$_2$ (5). A mixture of [Pt([9]aneS$_3$)-Cl$_2$] (98.0 mg, 0.220 mmol) and dppbe (110 mg, 0.246 mmol) was refluxed in 50 mL of CH_3NO_2 for 2.5 h. Metathesis to the hexafluorophosphate salt and ether diffusion resulted in yellow crystals of [Pt([9]aneS$_3$)(dppbe)](PF$_6$)$_2$ (111 mg, 0.100 mmol, 45.4%) which were suitable for X-ray diffraction (Found: C, 39.17; H, 3.41; S, 8.40. Calcd for $C_{36}H_{36}F_{12}P_4PtS_3$: C, 38.89; H, 3.26; S, 8.65%). IR (KBr): 3080, 3052, 3049, 3010, 2977, 2970, 2955, 2949, 1642, 1489, 1339, 1100, 837 (s, PF$_6^-$), 752, 696, 643, 564 cm^{-1}. Electronic spectrum (MeCN): three λ_{max} at 382 nm (ε = 200), at 297 nm (sh, ε = 7300) and at 264 nm (ε = 22000). ^{1}H-NMR (CD_3NO_2), δ (ppm): C$_6H_4$P$_2$: 8.26 (m, 2H), 7.48–7.33 (m, 2H); PPh_2: 7.84, 7.63 (m, 20 H); [9]aneS$_3$: complex AA′BB′ pattern at 2.93 and 2.53 (12 H); ^{13}C{^{1}H}-NMR (CD_3NO_2), δ (ppm): PPh_2: 134.9 (s, 4 C), 134.6 (m, 8 C), 131.1 (m, 8 C) and 130.7 (m, 4 C); C$_6H_4$P$_2$: 136.1 (s, 2 C), 135.2 (s, 2 C), 134.2 (m, 2 C); [9]aneS$_3$: 37.4 (s, 6 C). ^{195}Pt{^{1}H}-NMR (CD_3NO_2), δ ($\nu_{1/2}$): triplet at −4568 ppm (45 Hz) ($^1J_{PtP}$ = 3206 Hz). ^{31}P{^{1}H}-NMR (CD_3NO_2), δ: singlet at 45.97 ppm with ^{195}Pt satellites ($^1J_{PtP}$ = 3201 Hz).

Preparation of [Pt([10]aneS$_3$)(dppe)](PF$_6$)$_2$·CH$_3$NO$_2$ (6). A mixture of [Pt([10]aneS$_3$)Cl$_2$] (107 mg, 0.234 mmol) and dppe (95 mg, 0.238 mmol) was refluxed in 50 mL of CH_3NO_2 for 24 h. Metathesis to the hexafluorophosphate salt and ether diffusion resulted in yellow crystals of [Pt([10]aneS$_3$)(dppe)]-(PF$_6$)$_2$·CH$_3$NO$_2$ (111 mg, 0.0975 mmol, 41.7%) which were suitable for X-ray diffraction (Found: C, 35.88; H, 3.74; S, 8.47. Calcd for $C_{34}H_{41}F_{12}NO_2P_4PtS_3$: C, 35.86; H, 3.63; S, 8.45%). IR (KBr): 3060, 3013, 2981, 2914, 1559, 1437, 1382, 1333, 1105, 1002, 839 (s, PF$_6^-$), 748, 723, 683, 666, 580 cm^{-1}. The electronic absorption spectrum measured in acetonitrile showed two λ_{max} at 375 nm (ε = 204) and at 265 nm (ε = 32000). ^{1}H NMR (CD_3NO_2), δ (ppm): PPh_2: 7.87–7.82, 7.71–7.68 (broad m, 20 H); PCH_2CH_2P: 3.17–3.12 (m, 4 H); [10]aneS$_3$, α-methylene: 3.04–2.68 (broad, complex, overlapping peaks, m, 12 H); [10]aneS$_3$, β-methylene: 2.25–2.04 (broad m, 2 H). ^{13}C{^{1}H}-NMR (CD_3NO_2), δ (ppm): PPh_2: 134.9 (s, 4 C), 134.4 (m, 8 C), 131.2 (m, 8 C), 128.0 (m, 4 C); [10]aneS$_3$, α-methylene: 38.5, 32.7, 30.5 (s, 6 C); β-methylene: 24.8 (s, 1 C); PCH$_2$CH_2P: 31.1 (m, 2 C). ^{195}Pt{^{1}H}-NMR (CD_3NO_2), δ ($\nu_{1/2}$): triplet at −4602 ppm (38 Hz) ($^1J_{PtP}$ = 3224 Hz). ^{31}P{^{1}H}-NMR (CD_3NO_2), δ: singlet at 35.16 ppm with ^{195}Pt satellites ($^1J_{PtP}$ = 3219 Hz).

[Pt([9]aneS$_3$)(dppv)](PF$_6$)$_2$ (7). A mixture of [Pt([9]aneS$_3$)Cl$_2$] (98.0 mg, 0.220 mmol) and 1,2-bis(diphenylphosphino)ethylene (111 mg, 0.280 mmol) was refluxed in 50 mL of CH_3NO_2 for 2.5 h. Metathesis to the hexafluorophosphate salt and ether diffusion resulted in yellow crystals of [Pt([9]aneS$_3$)(dppv)]-(PF$_6$)$_2$ (104 mg, 0.0980 mmol, 44.5%) (Found: C, 36.14; H, 3.39; S, 8.80. Calcd for $C_{32}H_{34}F_{12}P_4PtS_3$: C, 36.20; H, 3.23; S, 9.06%). IR: 3058, 3013, 3011, 2956, 2929, 1588, 1520, 1426, 1305, 1184, 1099, 1025, 839 (s, PF$_6^-$), 735, 724, 693 cm^{-1}. Electronic spectrum (MeCN): two λ_{max} at 374 nm (ε = 306) and at 261 nm (ε = 24000). ^{1}H-NMR (CD_3NO_2), δ (ppm): PPh_2: 7.83, 7.68 (m, 20 H); PCHCHP: 7.39 (broad m, 2 H); [9]aneS$_3$: complex AA′BB′ pattern at 2.94 and 2.53 (12 H). ^{13}C{^{1}H}-NMR (CD_3NO_2), δ (ppm): PPh_2: 135.4 (s, 4 C), 134.5 (m, 8 C), 131.7 (m, 8 C), 126.7 (m, 4 C, ^1J(^{13}C–^{31}P) = 66 Hz); PCHCHP: 147.1 (m, 2 C); [9]aneS$_3$: 35.4 (s, 6 C). ^{195}Pt{^{1}H}-NMR (CD_3NO_2), δ ($\nu_{1/2}$): triplet at −4681 ppm (53 Hz) ($^1J_{PtP}$ = 3224 Hz). ^{31}P{^{1}H}-NMR (CD_3NO_2), δ: singlet at 42.09 ppm with ^{195}Pt satellites ($^1J_{PtP}$ = 3214 Hz).

Crystallographic data collection and processing

Bond distances and angles for the six structures appear in Table 2 and the details of data collection appear in Table 3. For the structures of compounds **1** and **2**, intensity data were collected on a Nonius CAD4 diffractometer, and the structures were solved using direct methods.[29] The intensity data of compounds **3**–**6** were collected on a Siemens SMART 1K CCD diffractometer[30,31] and their structures were solved using direct methods.[30]

CCDC reference numbers 180861–180866.

See http://www.rsc.org/suppdata/dt/b2/b202741k/ for crystallographic data in CIF or other electronic format.

Acknowledgements

This research was generously supported by grants from the Petroleum Research Fund, administered by the American Chemical Society, the Research Corporation, and the William L. Wheeler Center for Odor Research at the University of Tennessee at Chattanooga.

Table 3 Crystallographic data for [Pt(9S3)(dppe)]$(PF_6)_2$ (**1**), [Pt(9S3)(dppp)]$(PF_6)_2$ (**2**), [Pt(9S3)(dppb)]$(PF_6)_2$ (**3**), [Pt(9S3)(dpppe)]$(PF_6)_2$ (**4**), [Pt([9]aneS$_3$)(dppbe)]$(PF_6)_2$ (**5**), and [Pt([10]aneS$_3$)(dppe)]$(PF_6)_2$ (**6**)

	1	**2**	**3**	**4**	**5**	**6**
Empirical formula	$C_{32}H_{36}F_{12}P_4S_3Pt$	$C_{33}H_{38}F_{12}P_4S_3Pt$	$C_{34}H_{40}F_{12}P_4S_3Pt$	$C_{35}H_{42}F_{12}P_4S_3Pt$	$C_{36}H_{36}F_{12}P_4S_3Pt$	$C_{33}H_{36}F_{12}NO_2P_4S_3Pt$
M_r	1064.72	1077.81	1091.81	1105.84	1111.80	1121.78
Crystal system	Monoclinic	Monoclinic	Monoclinic	Monoclinic	Orthorhombic	Monoclinic
Space group	$P2_1/c$	$P2_1/c$	$P2_1/c$	$P2_1/c$	$Pca2_1$	$P2_1/n$
a/Å	11.179(2)	10.9130(13)	10.6367(1)	10.10719(4)	21.6418(9)	14.5881(1)
b/Å	17.711(2)	29.8500(22)	28.9211(3)	28.9211(3)	8.7316(4)	16.3447(2)
c/Å	20.511(3)	12.4053(16)	12.98850(1)	12.98850(1)	20.9904(8)	18.681(2)
α/deg	90	90	90	90	90	90
β/deg	103.480(16)	100.138(10)	99.665(1)	100.05(3)	90	105.528(1)
γ/deg	90	90	90	90	90	90
V/Å^3	3949.2(1)	3978.0(8)	3938.87(6)	3938.87(6)	3966.5(3)	4291.73(6)
Z	4	4	4	4	4	4
Radiation, λ/Å	0.71073	0.71073	0.71073	0.71073	0.71073	0.71073
d_{calcd}/g cm^{-3}	1.791	1.799	1.841	1.810	1.862	1.736
μ/mm^{-1}	10.50	10.43	3.968	3.852	3.942	3.648
T/K	295	295	293	293	173	300
No. of rflns	9228	9293	34807	25868	24135	27078
No. of unique rflns	6258	6631	9302	9578	9093	10157
R^a	0.040	0.040	0.0239	0.0467	0.0286	0.0301
$R_w{}^b$	0.053	0.053	0.0505	0.0626	0.0555	0.0750
GoF	1.91	1.91	1.053	0.954	0.949	1.083

^{a} $R = \Sigma||F_o| - |,F_c||/\Sigma|(F_o|$. ^{b} $R_w = [\Sigma w(|F_o| - |F_c|)^2/\Sigma wF_o)^2]^{1/2}$.

References and notes

1 For Part III, see G. J. Grant, D. F. Galas and D. G. VanDerveer, *Polyhedron*, 2002, **21**, 879.

2 A. J. Blake and M. Schröder, in *Advances in Inorganic Chemistry*, ed. A. G. Sykes, 1990, vol. 35, Academic Press, Inc., New York, p. 2; S. R. Cooper, *Acc. Chem. Res.*, 1988, **21**, 141; S. R. Cooper and S. C. Rawle, *Struct. Bonding (Berlin)*, 1990, **72**, 1; M. Schröder, *Pure Appl. Chem.*, 1988, **60**, 517; W. N. Setzer, E. L. Cacioppo, Q. Guo, G. J. Grant, D. D. Kim, J. L. Hubbard and D. G. VanDerveer, *Inorg. Chem.*, 1990, **29**, 2672; R. D. Adams, S. B. Falloon, K. T. McBride and J. H. Yamamoto, *Organometallics*, 1995, **14**, 1739; R. D. Adams and J. H. Yamamoto, *Organometallics*, 1995, **14**, 3704.

3 A. J. Blake, A. J. Holder, G. Reid and M. Schröder, *J. Chem. Soc., Dalton Trans.*, 1994, 627; A. J. Blake, R. O. Gould, A. J. Lavery and M. Schröder, *Angew. Chem., Int Ed. Engl.*, 1986, **25**, 274; S. J. Loeb and J. R. Mansfield, *Can. J. Chem.*, 1996, **74**, 1377; A. Pasini, S. Rizzato and D. De Cillis, *Inorg. Chim. Acta*, 2001, **315**, 196; E. L. M. Lempers and J. Reedjik, *Adv. Inorg. Chem.*, 1991, **285**, 249; H.-J. Drexler, I. Starke, M. Grotjahn, E. Kleinpeter and H.-J. Holdt, *Inorg. Chim. Acta*, 2001, **317**, 133.

4 A. J. Blake, R. O. Gould, A. J. Holder, T. I. Hyde, A. J. Lavery, M. O. Odulate and M. Schröder, *J. Chem. Soc., Chem. Commun.*, 1987, 118; A. J. Blake, R. D. Crofts and M. Schröder, *J. Chem. Soc., Dalton Trans.*, 1993, 2259.

5 G. J. Grant, N. S. Spangler, W. N. Setzer and D. G. VanDerveer, *Inorg. Chim. Acta*, 1996, **246**, 41.

6 T. W. Hambley, *Inorg. Chem.*, 1998, **37**, 3767.

7 The sum of the van der Waals radii for platinum(II) and sulfur is 3.50 Å; J. E. Huheey, E. A. Keiter and R. L. Keiter, *Inorganic Chemistry*, 4th edn., Harper Collins, New York, 1993, p. 292.

8 A. L. Balch, in *Homogenous Catalysis with Metal Phosphine Complexes*, ed. L. H. Pignolet, Plenum, New York, 1983, pp. 167–213; Y. Yamaguchi, M. Yabuki, T. Yamagishi, M. Kondo and S. Kitagawa, *Inorg. Chim. Acta*, 1997, **538**, 199.

9 J. R. Dilworth and N. Wheatley, *Coord. Chem. Rev.*, 2000, **199**, 89; J. Connolly, A. Genge, R. J. Pope, J. A. Simon and G. Reid, *Polyhedron*, 1998, **17**, 2331; W. Oberhauser, C. Bachmann, T. Stampfl, R. Haid, C. Langes, A. Reider and P. Bruggeller, *Inorg. Chim. Acta*, 1998, **274**, 143.

10 P. Dierkes and P. W. N. M. van Leeuwen, *J. Chem. Soc., Dalton Trans.*, 1999, 1520.

11 G. J. Grant, I. M. Poullaos, D. F. Galas, D. G. VanDerveer, J. D. Zubkowski and E. J. Valente, *Inorg. Chem.*, 2001, **40**, 564.

12 G. J. Grant, S. M. Carter, I. M. Poullaos and D. G. VanDerveer, *J. Organomet. Chem.*, 2001, **637–639**, 683. Special Issue for the 50th Anniversary of the Discovery of Ferrocene.

13 A. J. Blake, Y. V. Roberts and M. Schröder, *J. Chem. Soc., Dalton Trans.*, 1996, 1885.

14 H. Nikol, H.-B. Bürgi, K. I. Hardcastle and H. B. Gray, *Inorg. Chem.*, 1995, **34**, 6319.

15 G. J. Grant, C. G. Brandow, D. F. Galas, J. P. Davis, W. P. Pennington, J. D. Zubkowski and E. J. Valente, *Polyhedron*, 2001, **20**, 3333.

16 M. A. Bennett, J. K. Felixberger and A. C. Willis, *Gazz. Chim. Ital.*, 1993, **123**, 405; M. A. Bennett, A. J. Canty, J. K. Felixberger, L. M. Rendina, C. Sunderland and A. C. Willis, *Inorg. Chem.*, 1993, **32**, 1951; E. W. Abel, P. D. Beer, I. Moss, K. G. Orrell, V. Sik, P. A. Bates and M. B. Hurthouse, *J. Chem. Soc., Chem. Commun.*, 1987, 978.

17 T. G. Appleton, M. A. Bennett and I. B. Tompkins, *J. Chem. Soc., Dalton Trans.*, 1976, 439.

18 E. G. Hope, W. Levason and N. A. Powell, *Inorg. Chim. Acta*, 1986, **115**, 187.

19 W. Oberhauser, C. Bachmann and P. Brüggeller, *Inorg. Chim. Acta*, 1995, **238**, 35.

20 A. J. Blake, A. J. Holder, T. I. Hyde and M. Schröder, *J. Chem. Soc., Chem. Commun.*, 1989, 1433; G. J. Grant, J. P. Carpenter and W. N. D. G. Van Derveer, *Inorg. Chem.*, 1989, **28**, 4128.

21 D. C. Smith, C. M. Haar, E. D. Stevens, S. P. Nolan, W. J. Marshall and K. G. Moloy, *Organometalllics*, 2000, **19**, 1427.

22 We have obtained a correlation coefficient of 0.995 for a plot of $^1J(^{195}Pt–^{31}P)$ *vs.* the P–Pt–P chelate angle. A similar linear relationship exists between this coupling constant and the Pt–P–C angle.

23 A. M. Schuitema, M. Engelen, I. A. Koval, S. Gorter, W. L. Driessen and J. Reedijk, *Inorg. Chim. Acta*, 2001, **324**, 57.

24 G. J. Grant, S. M. Isaac, W. N. Setzer and D. G. VanDerveer, *Inorg. Chem.*, 1993, **32**, 429; G. J. Grant, B. M. McCosar, W. N. Setzer, J. D. Zubkowski and E. J. Valente, *Inorg. Chim. Acta*, 1996, **244**, 73; G.-H. Lee, *Acta Crystallogr., Sect. C*, 1998, **54**, 906.

25 L. M. Engelhardt, J. M. Patrick, C. L. Raston, P. Twiss and A. H. White, *Aust. J. Chem.*, 1984, **37**, 2193.

26 Although the Pt–S axial distances vary by as much as 1.0 Å in the eighteen crystal structures of the Pt–[9]aneS3 complexes, the sum of the three Pt–S distances is fairly constant and averages 7.55 (± 0.20) Å.

27 P. S. Pregosin, in *Transition Metal Nuclear Magnetic Resonance* ed. P. S. Pregosin, Elsevier, New York, 1991, p. 251; and references cited therein.

28 P. S. Pregosin, in *^{31}P and ^{13}C Nuclear Magnetic Resonance of Transition Metal Phosphine Complexes*, ed. P. Pregosin and R. W. Kunz, Springer-Verlag, New York, 1979.

29 NCRVAX—An Interactive Program System for Structure Analysis : E. J. Gabe, Y. Le Page, J.-P. Charland, F. L. Lee and P. S. White, *J. Appl Crystallogr.*, 1989, **22**, 384.

30 The programs used for data collection, solution and refinement of this structure are: SMART 5.054, SAINT$^+$ 6.01, SHELXTL 5.1, Bruker AXS, Madison, WI, USA, 1998–1999.

31 SADABS R: H. Blessing, *Acta Crystallogr. Sect. A*, 1995, **51**, 33.